THE JOURNAL OF PHYSICAL CHEMISTRY C

Article

pubs.acs.org/JPCC

In Silico Studies in Exploiting Weak Noncovalent C−H$^+$···π and π−π Interactions To Achieve Dual Properties: Hyperbasicity and Multiple Dihydrogen Storage Materials with Paracyclophane-Based Carbene Derivatives

Rabindranath Lo and Bishwajit Ganguly*

Computation and Simulation Unit (Analytical Discipline and Centralized Instrument Facility), CSIR-Central Salt & Marine Chemicals Research Institute, Bhavnagar, Gujarat, India 364 002

Supporting Information

ABSTRACT: This work reports that noncovalent interactions can be exploited to achieve hyperbasicity of a base. A new class of superbase has been identified using paracyclophane-based carbenes that possess a proton affinity (PA) value of 1251.4 kJ/mol at the M06-2X/6-311+G**//B3LYP/6-31+G* level of theory. Noncovalent interactions such as C−H$^+$···π and through-space π−π interactions amplify the basicity of such carbene systems by the stabilization of their protonated forms. These paracyclophane systems can be a suitable candidate for bis-protonation with the highest pK_a (MeCN) value of 50.1 to date. The side phenyl ring in paracyclophane systems that is not directly involved in C−H$^+$···π type interactions contributes to augment the basicity by through-space π−π interactions. The side ring of the paracyclophane system is involved in enhancement of the proton affinity of 19.3 kJ/mol via through-space π−π interaction. Molecular electrostatic potential (MESP) analysis shows that such noncovalent interactions can enhance the electron density at the reactive sites in suitably designed systems. The absolute minima of the MESP (V_{min}) located for these carbene systems correlate well with their calculated proton affinity values. The frontier molecular orbital energy differences (HOMO−LUMO) of such carbenes also correlate well with their proton affinity results. These paracyclophane-based carbene systems can be used for selective binding of lithium ions. Such lithium decorated systems can be exploited as a molecular container for the storage of multiple dihydrogen. This is the first example of the use of lithiated organic superbases as hydrogen storage material. The calculated conceptual density functional theory-based reactivity descriptors such as electronegativity, hardness, and electrophilicity indicate the stability of these H_2 trapped molecules. The calculated desorption energies per H_2 molecule (ΔE_{DE}) also indicate the recyclable property of the hydrogen storage materials.

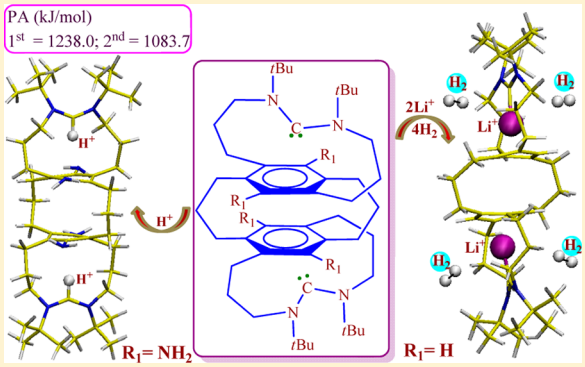

1. INTRODUCTION

The effectiveness of neutral organic superbases as catalysts have been explored in modern organic chemistry in recent times.[1,2] Organic superbases such as amidines, guanidines, and phosphazenes are considered as an important class of reagent in the field of current organic chemistry.[3−27] The requirement of mild reaction conditions and better solubility of organic superbases in most of the organic solvent makes these superbases efficient candidates compared to their inorganic counterparts.[28,29] Organic superbases possess environmentally friendly recyclable properties.[30] Besides possessing such important properties, the organic superbases are often employed as one of the components in CO_2 trapping agents.[31−36] Strong organic bases such as diazabicyclo[5.4.0]-undec-7-ene (DBU), 1,5,7-triazabicyclo[4.4.0]-dec-5-ene (TBD), 1,5-diazabicyclo[4.3.0]-non-5-ene (DBN), and polycyclic diazatricyclo[5.3.1.1^{2,6}]dodecane in combination with alcohol were able to capture CO_2 for the formation of the corresponding amidinium/guanidinium alkyl carbonate salts.[15,34] As a result, the design of novel and efficient organic superbases is an active field of research.

We have reported herein a series of carbene superbases based on the [3.3] paracyclophane system. The design of novel organic superbases with minimum functional groups is synthetically attractive by exploiting the noncovalent C−H$^+$···π interactions.[13] Such noncovalent interactions stabilize the systems by ∼125.5 kJ/mol.[37] Herein, we have utilized weak noncovalent interactions in designing a new class of organic superbases where an acyclic carbene [:C(NR$_2$)$_2$] unit connects with the phenyl ring of the paracyclophane systems through propyl chains (Scheme 1). The through-space π−π interactions[38,39] enhance the proton affinity by the side phenyl ring

Received: June 24, 2013
Revised: August 16, 2013
Published: August 22, 2013

Scheme 1

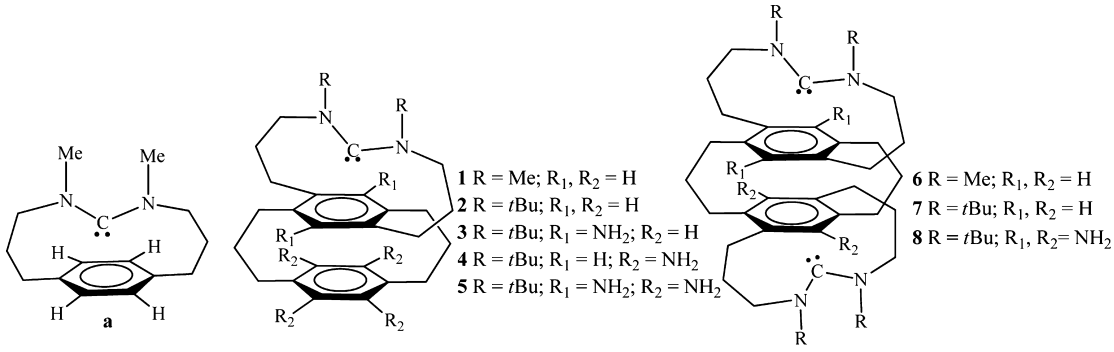

of the paracyclophane systems along with C−H$^+$···π type interactions to achieve hyperbasicity.[40] Such strategies would help to attain higher basicities by avoiding large functionalizations in basic fragments, which are also synthetically demanding.[11,12,17−19,21]

This paracyclophane-based carbene superbase also can be extended for the bis-protonation study (Scheme 1). The second protonation site of these carbene-based scaffolds enables bis-protonation, examples of which are rare in the literature.[4,13,15,27] The first proton affinity of the designed superbase is in the range of a hyperbase (compounds that have a proton affinity > 300 kcal mol^{-1} = 1255.2 kJ mol^{-1}),[12,13,21,40] and the second proton affinity is highest in terms of bis-proton affinity reported in the literature to date. This study reports the first example exhibiting the use of an organic superbase as a molecular container for hydrogen storage (H_2).

Hydrogen energy is considered as an ideal energy source due to its highly abundant and environmentally friendly nature.[41,42] The main source for the production of molecular hydrogen comprises the renewable energy resources, and it discards the production of different hazardous byproducts.[43] The major problem in the field of hydrogen energy is economic and safe hydrogen storage.[44] A number of materials have been used in hydrogen adsorption such as carbon, boron-based nanomaterials,[45−47] alanates,[48] clathrates,[49] borates,[50] zeolites,[51] metal hydrides,[52] metal−organic frameworks (MOFs),[53,54] covalent-organic frameworks (COFs),[55] zeolitic-imidazole frameworks (ZIFs),[56] porous silica, etc.[57] For an efficient hydrogen storage material, the manufacture process should be economical, and the storage materials should have a high gravimetric or volumetric uptake capacity and fast kinetics for adsorption and desorption processes.[58,59] The probing of new material for hydrogen storage has been of immediate interest.

The studies have been directed to improve the hydrogen binding energy by incorporating metal or charged sites such as Li or transition metals in hydrogen storage material.[60−65] The electropositive Li^+ ion binds strongly with molecular hydrogen. Consequently, the design of effective and energetically stable Li-decorated compounds is desirable.

We have reported here that these superbasic carbene scaffolds can be used as an efficient hydrogen storage material. These molecular scaffolds have two binding sites and show selective preference for small alkali metal cation such as the lithium ion. This will enable the spontaneous binding of molecular hydrogen in both sides with the electropositive lithium metal ions.

2. COMPUTATIONAL SECTION

Calculations were performed for compounds **1**−**8** with the density functional theory using Becke's three-parameter hybrid functional with correlation formula of Lee, Yang, and Parr (B3LYP).[66,67] All these species were fully optimized with the 6-31+G* basis set,[68] and harmonic vibrational frequency calculations were used to confirm the stationary points. The reliability of the B3LYP level for the calculations of the proton affinities for the divalent carbenes has been examined previously.[13] Single point calculations are performed with the B3LYP/6-311+G** level of theory. Further, we have employed the M06-2X/6-311+G** level of theory to calculate the energies for these optimized carbene systems as M06-2X DFT functional considers the dispersion interactions more accurately for nonbonded interactions.[69]

Solvent effects are taken into account by means of the polarizable continuum model (PCM)[70−74] through single-point energy calculations at the B3LYP/6-311+G** level of theory (using the gas-phase optimized geometries). The pK_a value of the acid BH^+ is calculated using the following relation,

$$pK_a = \Delta G_{sol}/2.303RT$$

where

$$\Delta G_{sol} = \Delta G_{gas} + \Delta\Delta G_{solv} + \Delta G_{corr}$$

ΔG_{gas} is the Gibbs free energy change of the reaction in the gas phase, and $\Delta\Delta G_{solv}$ is the difference in solvation free energies (ΔG_{solv}) between products and reactants. ΔG_{corr} is the correction associated with the change in standard state from gas phase (1 atm) to solution (1 mol/L), and its value at 298.15 K is 1.89 kcal/mol.[75]

Now ΔG_{sol} can be expressed as

$$\Delta G_{sol} = G_{gas}(B) + \Delta G_{solv}(B) + G_{gas}(H^+) + \Delta G_{solv}(H^+) - G_{gas}(BH)^+ - \Delta G_{solv}(BH)^+ + 1.89$$

Here, the value of Gibbs free energy of the proton in the gas phase is set to −6.28 kcal/mol using translational entropy calculated according to the well-known Sackur−Tetrode equation[76] and the value of Gibbs free energy of proton in acetonitrile solvent phase taken as −250.76 kcal/mol.[77]

The ΔG_{solv} values in B3LYP/6-31+G* optimized geometry with UAHF radii and "scfvac" keyword using acetonitrile (ε = 36.64) as a solvent.[78,79] The reliability of this method for pK_a calculations has already been shown in earlier reports.[79] Both electrostatic and nonelectrostatic (i.e., cavitation, repulsion, and dispersion) terms were included in the calculation of ΔG_{solv} values.

dx.doi.org/10.1021/jp406234f | J. Phys. Chem. C 2013, 117, 19325−19333

For the determination of the stability of carbenes in solvent medium, carbenes are optimized at the B3LYP/6-31+G* level of theory in acetonitrile medium with the PCM solvation model, and then single point energies are calculated at the M06-2X/6-311+G** level of theory in singlet and triplet states.

The molecular electrostatic potential (MESP) was calculated using eq 1 where Z_A was the charge on nucleus A, situated at R_A and $\rho(r')$ is the electron density.[80]

$$V(\mathbf{r}) = \sum_{A}^{N} \frac{Z_A}{|r - R_A|} - \int \frac{\rho(r')d^3r'}{r - r'} \quad (1)$$

In general, electron-rich regions are shown by a highly negative MESP, whereas electron-deficient regions are characterized by positive MESP.[81−85] The most negative valued point (V_{min}) in electron-rich regions can be determined from the MESP topography calculation.[86−88] MESP calculations have been performed at the M06-2X/6-311+G** level of theory.

The geometries are optimized at the M06-2X/6-31+G* level of theory for the calculation of lithium and sodium affinity calculations. We have employed the M06-2X/6-311+G** level of theory to calculate the energies for these optimized geometries. For the calculation of interaction energy per H_2 molecule and desorption energy per H_2 molecule, the following expressions have been used:[64]

Interaction energy/H_2 molecule

$$\Delta E = [E_{S(H_2)_n} - (E_s + nE_{H_2})]/n$$

n = no. of molecular H_2

Desorption energy

$$\Delta E_{DE} = E_{H_2} + \left(\frac{1}{m}\right)[E_{S(H_2)_{n-m}} - E_{S(H_2)_n}]$$

where n, m = no. of H_2 molecules, and S is the hydrogen-trapped systems.

The absolute electronegativity (χ) and the absolute hardness (η) are calculated by the formula, χ = (IP + EA)/2 and η = (IP − EA), respectively.[64] The ionization potential (IP) was calculated as the energy difference between the nonoptimized cation-radical structure and the ground state structure and the electron affinity (EA) was calculated as the energy difference between the anion-radical and ground state. Electrophilicity (ω) is defined as

$$\omega = \frac{\chi^2}{2\eta}$$

Quantum chemical calculations were performed using Gaussian 03, Revision E.01 program,[89] while the calculations at M06-2X level have been performed using the Gaussian 09 program.[90]

3. RESULTS AND DISCUSSION

The explored compounds are illustrated in Scheme 1. Herein, we have employed the M06-2X/6-311+G** level of theory to calculate the energies for these carbene systems, and the proton affinities discussed in this study are calculated at this level of theory. The proton affinity values calculated at the M06-2X level are slightly lower compared to the B3LYP level (Table 1). The M06-2X/6-311+G**//B3LYP/6-31+G* calculated results illustrate that the proton affinity of **1** is 1179.5 kJ/mol (Table 1). This proton affinity (PA) value is much higher than the proton affinity of a threshold organic superbase (compounds that have a PA > 1000 kJ/mol = 239 kcal/mol) and comparable with highly basic imines and phosphazene systems.[91,92] The role of the paracyclophane moiety to enhance the basicity in these carbene systems is clearly shown from the calculated proton affinity values. By introducing the paracyclophane attached with alkyl chains of simple :$C(NMe_2)_2$, the proton affinity value increases by ∼55.7 kJ/mol compared to simple carbene :$C(NMe_2)_2$.[77] In the protonated form of carbene **1**, the proton is more stabilized by the paracyclophane system compared to the single phenyl ring that is reflected in the calculated PA values.[13,38,39] The side phenyl ring in **1** helps to augment the basicity by 19.3 kJ/mol at the M06-2X/6-311+G** level of theory through $\pi-\pi$ interactions compared to the case where such side rings are absent (**a**) (Figure 1). These calculated results suggest that the noncovalent $CH^+\cdots\pi$ interaction contributes to increase the proton affinity of the carbene **1** by ∼36.4 kJ/mol. The MESP analysis shows that the presence of the side phenyl ring in paracyclophane systems increases the V_{min} value in the region between the carbene carbon and phenyl ring of **1** (−380.7 kJ/mol) compared to single phenyl ring systems (**a**) (−370.3 kJ/mol) (Figure 1). Further, the geometrical parameters also corroborate that the distance between the two phenyl rings in paracyclophane is reduced upon the protonation process (Table S1, Supporting Information). This is expected as the repulsion between the π-planes is reduced for such a protonation process.

Table 1. B3LYP/6-311+G//B3LYP/6-31+G* Calculated Proton Affinities (kJ/mol) and pK_a (MeCN) for 1−8 in the Gas Phase at 298.15 K[a]**

	proton affinities[b] (kJ/mol)		
compound	first	second	pK_a (MeCN)
1	1189.5 (1179.5)		46.7
2	1217.5 (1212.5)		48.5
3	1236.4 (1230.9)		50.4
4	1237.6 (1235.5)		48.7
5	1256.0 (1251.4)		51.5
6	1197.9 (1191.6)	1035.1 (1015.5)	45.5, 44.9
7	1228.0 (1226.7)	1081.1 (1069.0)	48.2, 47.8
8	1242.6 (1238.0)	1097.5 (1083.7)	50.5, 50.1

[a]M06-2X/6-311+G**//B3LYP/6-31+G* calculated proton affinities are given in parentheses. [b]Zero-point energy corrected.

The proton affinity of **1** can further be increased upon the introduction of *t*Bu groups in aminomethyl positions (Scheme 1 and Table 1). The electron donating effect of *t*Bu groups can enhance the electron density at the carbene carbon center through an inductive effect. The MESP surface suggests that the V_{min} is larger in **2** (−391.6 kJ/mol) compared to **1** (−380.7 kJ/mol) (Figure 1). The calculated PA value for **2** was found to be 33.0 kJ/mol higher than that of **1** (Table 1).

We have examined the influence of substituents on the phenyl rings of paracyclophane with a suitable electron donating group. We have modeled the electron donating group with the (−NH_2) group in the phenyl rings (Scheme 1). In carbene **3** and **4**, -NH_2 groups are substituted at the main phenyl ring and the side phenyl ring of the paracyclophane system, respectively. The combined effect of induction and π-electron conjugation of the amine group can contribute to increase the electron density in the π cloud of the phenyl rings.[93] Similar substituted paracyclophane derivatives have been synthesized and reported in the literature.[94,95] Carbene **4** shows slightly higher proton affinity value compared to **3** (Table 1), and the calculated PA values suggest that the

dx.doi.org/10.1021/jp406234f | J. Phys. Chem. C 2013, 117, 19325−19333

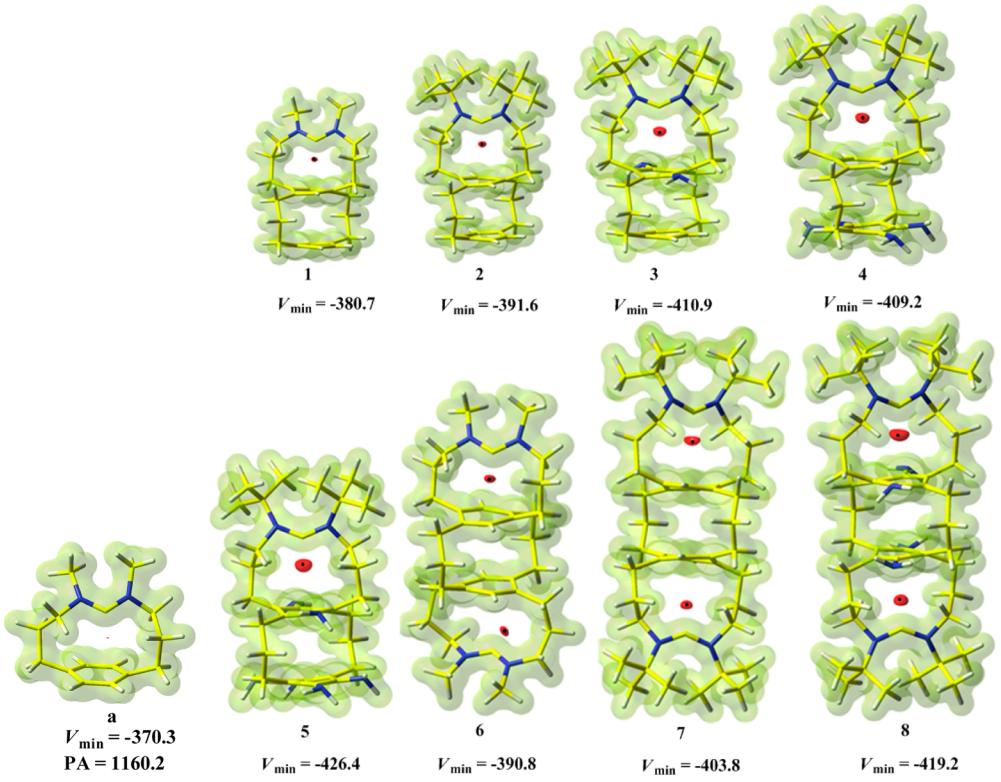

Figure 1. Representation of the MESP isosurface at −370.3 kJ/mol. V_{min} and proton affinity (PA) values are given in kJ/mol.

substitutions at the side ring can enhance the PA by through-space $\pi-\pi$ interactions.[39] The introduction of electron donating -NH_2 groups in the main and side phenyl rings of the paracyclophane system **3** and **4** augments the proton affinities by 18.4 and 23.0 kJ/mol, respectively, than the unsubstituted paracyclophane system **2** (Table 1). However, the PA value is enhanced remarkably in **5** where both the phenyl rings are substituted with -NH_2 groups. Carbene **5** showed a PA value of 1251.4 kJ/mol, which is the range of a hyperbase (Table 1). This is the first example of carbene systems that show PA ∼300 kcal/mol or 1255.2 kJ/mol.

The MESP results show that the electron-rich region residing in between the carbene carbon and the phenyl ring increases on going from **1** to **5** (Figure 1). The electron-dense regions are anticipated to show a highly negative MESP. These MESP results suggest that the incoming proton is stabilized in the region between the carbene carbon and the phenyl ring. The PA values for these compounds correlate well with the V_{min} (Figure S1, Supporting Information).

This molecular scaffold has been considered further for bis-protonation study (Scheme 1 and carbenes **6**−**8**). The two divalent carbon(II) units were protonated sequentially to obtain the first and second proton affinities. It is reported that the second proton affinity with nitrogen bases are much lower than that of the first protonation.[4,15] The first PA calculated for **6** is 1191.6 kJ/mol, and the second PA is 1015.5 kJ/mol. The calculated second proton affinity is comparable with the proton affinity of prototype 1,8-bis(dimethylamino)naphthalene (DMAN).[91] By introducing the second carbene unit in the paracyclophane system of carbene **1**, the PA value is increased by ∼12.1 kJ/mol (Table 1). The MESP analysis shows that the introduction of the second carbene unit in **6** increases the V_{min} value in the region between the carbene carbon and phenyl ring of **6** (−390.8 kJ/mol) compared to **1** (−380.7 kJ/mol) (Figure 1). Furthermore, the greater reduction of $\pi-\pi$ repulsion upon protonation in the paracyclophane moiety in **6** also contributes to enhancement of the PA values (Table S1, Supporting Information).[38,39] The PA value was found to be enhanced by introducing *t*Bu in this molecular scaffold (Scheme 1). Carbene **7** showed the first PA of 1226.7 kJ/mol, and the second PA is 1069.0 kJ/mol (Table 1).

We have extended the study with further substitution of the phenyl rings in such paracyclophane systems (Scheme 1). The introduction of -NH_2 groups in **8** increases the V_{min} value significantly in carbene **8** (−419.2 kJ/mol) compared to **7** (−403.8 kJ/mol) (Figure 1). Therefore, the PA values are found to be enhanced in the amine-substituted carbene **8** compared to **7**. The amine substituted carbene **8** shows the highest second PA in the series. This second PA value is much higher than normal NHCs.[96] The reported second PA value of the 4,8,9,10-tetramethyl-4,8,9,10-tetraazatricyclo [5.1.1.1^{3,5}]-]decane system was found to be 697.9 kJ/mol, and the polycyclic diazatricyclo dodecane system showed the second PA value of 1071.5 kJ/mol.[4,15] To the best of our knowledge, the second proton affinity calculated for **8** (1083.7 kJ/mol) is much higher than the prototype commonly used superbase (DMAN) and the highest second PA reported to date.[4,13,15,27]

We have reported the pK_a of carbene superbases using a similar level of theory, which has been examined against the available experimental data.[13] We have calculated the pK_a values of the designed carbene superbases (**1**−**8**) in acetonitrile as this particular solvent is commonly used for such purposes. The basicity of organic superbases is measured in lower acidic and aprotic solvents of low and medium polarity.[97] The level of theory employed here to examine the pK_a showed good agreement with some of the observed pK_a values.[13] The pK_a value of **1** is 46.7. The calculated results show that the most basic carbene **5** exhibits a pK_a of 51.5 and has been found to be

dx.doi.org/10.1021/jp406234f | J. Phys. Chem. C 2013, 117, 19325−19333

much higher than the reported pK_a values (40−46.9) of known superbases.[11,12,17,18,20] The second pK_a value is reported for the designed superbases up to 50.1, which is the highest second pK_a reported to date. The calculated second pK_a values calculated for **6**−**8** are comparable to the first pK_a values due to the greater stabilization of the bis-cationic form of carbenes in the solvent medium compared to the corresponding neutral and monocationic forms.[98] It is to note that the solvation seems to affect the C−H$^+$···π interactions;[99] hence, some variations might be seen in the calculated and experimentally determined pK_a values of these systems.

We have calculated the energy difference between the singlet and triplet states ($E_{S\text{-}T}$) of the carbenes in acetonitrile medium to determine the stability of such systems in solvent medium. The $E_{S\text{-}T}$ value indicates the nature and reactivity of carbene systems.[13,16,100] The calculated value of $E_{S\text{-}T}$ for divalent carbene **1** is 180.8 kJ/mol, which suggests the higher relative stability of the singlet state of **1** compared to the triplet state (Table S2, Supporting Information). The greater preferences of singlet states over triplet states are also found for dicarbene system **6**. These calculated results suggest that the divalent monocarbene and dicarbene can be used as possible synthetic targets.

The energies of the frontier orbitals in the carbenes also provide information about the reactivity and stability of these systems. In the highest occupied molecular orbital (HOMO), the lone-pair is localized on the central carbon atom (Figure S2, Supporting Information). Compound **5** shows the highest HOMO energy (−5.05 eV) in the series, which suggests its higher reactivity compared to the other studied carbene molecules (Table S3, Supporting Information). The calculated proton affinity values correlate this observation (Table 1). A good correlation between calculated PA and E_{HOMO} was observed with a high correlation coefficient value of 0.98 (Figure S3, Supporting Information). The HOMO−LUMO energy gap (HLG) also explains the reactivity and stability of the carbene molecules. The correlation between the calculated PA and the HOMO−LUMO energy gap of the carbene systems also shows a good correlation with high correlation coefficient (Figure S4, Supporting Information).

The calculated results show that the designed carbene derivatives with high basicities can be useful in organic synthesis, green chemistry, etc.[1,2] Here, we have taken a new approach to exploit these carbene derivatives as materials for hydrogen storage. In recent years, the lithium decorated organic molecules have been tested for efficient hydrogen adsorption.[60−65] Lithium ion doped substituted borazines, star-like clusters, and superalkali systems have been used as potential hydrogen trapping agents.[60−65] We have shown use of such carbene superbases for selective binding of lithium ions and effective storage materials for hydrogen. The advantage of using these designed carbenes is that these superbases can accommodate two metal ions at reasonable distances and hence can bind with multiple dihydrogens. The analysis of the geometrical parameters of these carbenes shows that the distance between the carbene carbon and the center of the phenyl ring is in the range of 3.200−3.600 Å. This distance is appropriate for the efficient noncovalent interaction of proton with the aromatic rings. We have decided to explore the binding affinity of the smallest alkali metal ion, i.e., Li^+ (ionic radius 0.76 Å), with these paracyclophane-derived systems. The calculated binding energies suggest that these carbene scaffolds have a tendency to bind strongly with lithium ion, and carbene **5** shows the highest binding energy in the series (Table 2). These large interaction energies point out the stability of the

Table 2. Complexation Energies of Different Carbenes at M06-2X/6-311+G//M06-2X/6-31+G* Level of Theory[a]**

carbenes	B.E. (Li^+)	B.E. (Na^+)	ΔE (Li^+/Na^+)
1	−364.8	−251.5	113.3
2	−386.2	−286.6	99.6
5	−436.0	−348.9	87.1
6 (mono)	−364.4	−256.5	107.9
6 (bis)	−169.5	−81.2	88.3
7 (mono)	−405.0	−305.0	100.0
7 (bis)	−188.7	−98.3	90.4
8 (mono)	−423.4	−348.5	74.9
8 (bis)	−214.2	−140.2	74.0

[a]Energies in kJ/mol.

complexes toward dissociation.[65] The greater electronegativity of the carbene carbon atom compared to lithium makes the C−Li bonds polar in nature. The NBO charge analysis also shows the higher positive charge on the lithium center compared to the carbon atom (Table S4, Supporting Information). We have further examined the binding affinity of sodium cation (ionic radius 1.02 Å), which however showed much lower binding energies with these carbene systems (Table 2). The stronger binding of Li^+ ion with these carbene scaffolds prompted us to evaluate the adsorption of hydrogen molecules with such well-organized lithiated systems.

The lithiated carbene compounds (**1**, **2**, **5**−**7**) are examined for hydrogen storage materials. The optimized H_2 trapped lithiated carbenes (**6**−**7**) are given in Figure 2. The calculated

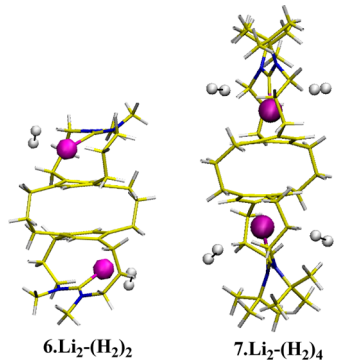

Figure 2. Geometries of hydrogen trapped lithiated carbenes at the M06-2X/6-31+G* level of theory. [Yellow = carbon; blue = nitrogen; pink = lithium; and white = hydrogen].

results show that the lithiated carbene **1** trapped molecular hydrogen with an interaction energy of −15.1 kJ/mol per H_2 molecule (Table 3). The larger negative ΔH values also indicate the exothermicity of the H_2 trapping process (Table 3). The calculated desorption energies per H_2 molecule (ΔE_{DE}) also suggest the recyclable property of the hydrogen storage materials.[64] The lithiated carbenes **1** and **6** show comparatively higher interaction energy compared to other systems.[62,64,65] The favorable interactions occur in these cases due to the presence of high positive charge on Li and trap the H_2 molecule through ion-quadrupole and ion-induced dipole interactions (Table S4, Supporting Information).[64,65,101] In compound **1**, the hydrogen atom resides at a distance of 2.16 Å from the Li^+

dx.doi.org/10.1021/jp406234f | J. Phys. Chem. C 2013, 117, 19325−19333

Table 3. Interaction Energy Per Hydrogen Molecule (ΔE), Desorption Energy Per H_2 (ΔE_{DE}) Molecule, Reaction Enthalpy (ΔH) and HOMO−LUMO Gaps for Hydrogen Trapped Lithiated Carbenes[a]

	ΔE	ΔE_{DE}	ΔH	HOMO−LUMO gap (eV)
1·Li + H_2 = **1**·Li−H_2	−15.1	15.1	−5.0	6.61
2·Li + H_2 = **2**·Li−H_2	−10.9	10.9	−2.1	6.40
2·Li + $2H_2$ = **2**·Li-$(H_2)_2$	−10.0	9.2	−1.7	6.40
5·Li + H_2 = **5**·Li−H_2	−10.9	10.9	−2.5	5.75
5·Li + $2H_2$ = **5**·Li-$(H_2)_2$	−10.5	10.0	−2.5	5.75
6·Li_2 + H_2 = **6**·Li_2−H_2	−17.2	17.2	−5.4	6.70
6·Li_2 + $2H_2$ = **6**·Li_2-$(H_2)_2$	−16.7	16.3	−5.0	6.69
7·Li_2 + H_2 = **7**·Li_2−H_2	−10.5	10.5	−2.9	5.63
7·Li_2 + $2H_2$ = **7**·Li_2-$(H_2)_2$	−10.0	10.0	−2.5	5.61
7·Li_2 + $3H_2$ = **7**·Li_2-$(H_2)_3$	−10.0	10.0	−2.5	5.63
7·Li_2 + $4H_2$ = **7**·Li_2-$(H_2)_4$	−9.6	8.8	−2.1	5.61

[a]Energies are in kJ/mol.

ion (Table S4, Supporting Information). However, the distance is reduced to 2.10 Å in compound **6**, which is reflected in the higher binding energy calculated for **6** compared to **1** (Tables 3 and S4, Supporting Information). In compound **7**, we have explored the possibility of hydrogen adsorption with four molecular hydrogens (Figure 2). The calculated interaction energies slightly decrease with the increase in the number of adsorbed hydrogen molecule (Table 3).[64,65] NBO charge analysis showed that the positive charge is reduced in the H_2 trapped molecules (Table S4, Supporting Information).[65,102]

The calculated global reactivity descriptors indicate the stability of H_2 trapped molecules according to both the maximum hardness principle and the minimum electrophilicity principle.[103,104] After H_2 binding, the hardness (η) value of the lithiated carbene **1** is increased and electrophilicity (ω) value is decreased, which facilitates the H_2 trapping process (Table S5, Supporting Information). The calculated HOMO−LUMO gap for these hydrogen trapped lithiated carbenes shows that the higher binding energy is directly related to the larger gap between the frontier molecular orbitals (Table 3). The frontier molecular orbital pictures show that the orbital symmetry of the parent and the molecular H_2-bound system **6** are the same, which explained the retaining of the molecular nature in the trapped hydrogen (Figure 3).

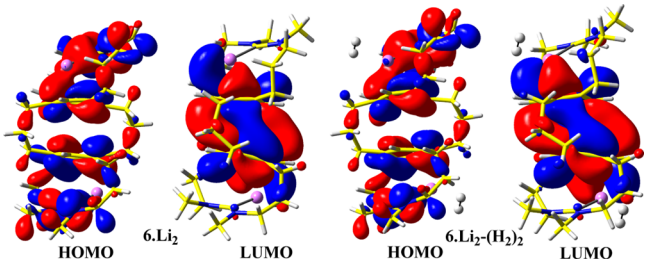

Figure 3. Frontier molecular orbitals of hydrogen trapped lithiated carbenes at the M06-2X/6-311+G** level.

4. CONCLUSIONS

In this study we have reported newly derived paracyclophane-based carbene molecular architectures to achieve hyperbasicity with the weak noncovalent C−H^+···π and through-space π−π interactions. Through-space π−π interaction was observed with the side phenyl ring of the paracyclophane system, which enhances the proton affinity by ∼19.3 kJ/mol. Further, the side phenyl ring of the paracyclophane-based carbene system can be utilized for bis-protonation. The second protonation site of the superbase (**8**) possesses the highest pK_a value (50.1), which is a rare example in the literature. The MESP analysis shows that noncovalent interactions can augment the basicity in suitably designed systems. The absolute minima of the MESP (V_{min}) for these carbene systems suggest that the V_{min} located for carbene carbon and phenyl ring of **1** (−380.7 kJ/mol) is higher compared to single phenyl ring systems (**a**) (−370.3 kJ/mol) due to the presence of the side phenyl ring in paracyclophane systems. Further, the V_{min} value located for these carbene systems correlated with their calculated proton affinity values. This is an example where we have shown that these superbases can be exploited as molecular containers for the storage of multiple dihydrogen. The variation of different global reactivity descriptors indicates the stability of these H_2 trapped molecules. The maximum hardness principle and the minimum electrophilicity principle also show the feasibility of the H_2 trapping process. We hope that this information will stimulate chemists to exploit the use of organic superbases for hydrogen storage materials besides their many other applications.

■ ASSOCIATED CONTENT

Supporting Information

Cartesian coordinates of all the geometries, including electronic energies. This material is available free of charge via the Internet at http://pubs.acs.org.

■ AUTHOR INFORMATION

Corresponding Author

*E-mail: ganguly@csmcri.org.

Notes

The authors declare no competing financial interest.

■ ACKNOWLEDGMENTS

One of the authors R.L. is thankful to UGC, New Delhi, India, for awarding a senior research fellowship. B.G. thanks (MSM, SIP, CSIR, New Delhi) and DST, New Delhi, for financial support. We are also thankful to the reviewers for their suggestions and comments that have helped us to improve the paper.

■ REFERENCES

(1) *Superbases for Organic Synthesis*; Ishikawa, T., Ed.; Wiley: Chichester, West Sussex, 2009.

(2) Hirono, Y.; Kobayashi, K.; Yonemoto, M.; Kondo, Y. Metal-free deprotonative functionalization of heteroaromatics using organic superbase catalyst. *Chem. Commun.* **2010**, *46*, 7623−7624 and references therein.

(3) Bachrach, S. M.; Wilbanks, C. C. Using the Pyridine and Quinuclidine Scaffolds for Superbases: A DFT Study. *J. Org. Chem.* **2010**, *75*, 2651−2660.

(4) Estrada, E.; Simón-Manso, Y. Rational Design and First Principles Studies Toward the Discovery of a Small and Versatile Proton Sponge. *Angew. Chem., Int. Ed.* **2006**, *45*, 1719−1721.

(5) Maksić, Z. B.; Kovačević, B.; Vianello, R. Advances in Determining the Absolute Proton Affinities of Neutral Organic Molecules in the Gas Phase and Their Interpretation: A Theoretical Account. *Chem. Rev.* **2012**, *112*, 5240−5270.
(6) Singh, A.; Ganguly, B. DFT Studies toward the Design and Discovery of a Versatile Cage-Functionalized Proton Sponge. *Eur. J. Org. Chem.* **2007**, 420−422.
(7) Singh, A.; Ganguly, B. Strategic design of small and versatile bicyclic organic superbases: a density functional study. *New J. Chem.* **2008**, *32*, 210−213.
(8) Singh, A.; Ganguly, B. Rational Design and First-Principles Studies toward the Remote Substituent Effects on a Novel Tetracyclic Proton Sponge. *J. Phys. Chem. A* **2007**, *111*, 6468−6471.
(9) Maksić, Z. B.; Kovačević, B. Absolute proton affinity of some polyguanides. *J. Org. Chem.* **2000**, *65*, 3303−3309.
(10) Vianello, R.; Kovačević, B.; Maksić, Z. B. In search of neutral organic superbases—iminopolyenes and their amino derivatives. *New J. Chem.* **2002**, *26*, 1324−1328.
(11) Margetić, D.; Ishikawa, T.; Kumamoto, T. Exceptional Superbasicity of Bis(guanidine) Proton Sponges Imposed by the Bis(secododecahedrane) Molecular Scaffold: A Computational Study. *Eur. J. Org. Chem.* **2010**, 6563−6572 and references therein.
(12) Peran, N.; Maksić, Z. B. Polycyclic croissant-like organic compounds are powerful superbases in the gas phase and acetonitrile—a DFT study. *Chem. Commun.* **2011**, *47*, 1327−1329.
(13) Lo, R.; Ganguly, B. First principle studies toward the design of a new class of carbene superbases involving intramolecular H···π interactions. *Chem. Commun.* **2011**, *47*, 7395−7397.
(14) Lo, R.; Ganguly, B. Exploiting propane-1,3-diimines as building blocks for superbases: a DFT study. *New J. Chem.* **2011**, *35*, 2544−2550.
(15) Lo, R.; Singh, A.; Kesharwani, M. K.; Ganguly, B. Rational design of a new class of polycyclic organic bases bearing two superbasic sites and their applications in the CO_2 capture and activation process. *Chem. Commun.* **2012**, *48*, 5865−5867.
(16) Biswas, A. K.; Lo, R.; Ganguly, B. First Principles Studies toward the Design of Silylene Superbases: A Density Functional Theory Study. *J. Phys. Chem. A* **2013**, *117*, 3109−3117.
(17) Kovačević, B.; Barić, D.; Maksić, Z. B. Basicity of exceedingly strong non-ionic organic bases in acetonitrile —Verkade's superbase and some related phosphazenes. *New J. Chem.* **2004**, *28*, 284−288.
(18) Kovačević, B.; Maksić, Z. B. High basicity of tris-(tetramethylguanidinyl)-phosphine imide in the gas phase and acetonitrile—a DFT study. *Tetrahedron Lett.* **2006**, *47*, 2553−2555.
(19) Kovačević, B.; Maksić, Z. B. High basicity of phosphorus−proton affinity of tris-(tetramethylguanidinyl)phosphine and tris-(hexamethyltriaminophosphazenyl)phosphine by DFT calculations. *Chem. Commun.* **2006**, 1524−1526.
(20) Schwesinger, R.; Hasenfratz, C.; Schlemper, H.; Walz, L.; Peters, E.-M.; Peters, K.; von Schnering, H. G. How Strong and How Hindered Can Uncharged Phosphazene Bases Be? *Angew. Chem., Int. Ed.* **1993**, *32*, 1361−1363.
(21) Despotović, I.; Kovačević, B.; Maksić, Z. B. Hyperstrong Neutral Organic Bases: Phosphazeno Azacalix[3](2,6)pyridines. *Org. Lett.* **2007**, *9*, 4709−4712.
(22) Despotović, I.; Maksić, Z. B.; Vianello, R. Design of Brønsted Neutral Organic Bases and Superbases by Computational DFT Methods: Cyclic and Polycyclic Quinones and [3]Carbonylradialenes. *Eur. J. Org. Chem.* **2007**, 3402−3413 and references therein..
(23) Kovačević, B.; Despotović, I.; Maksić, Z. B. In quest of strong neutral organic bases and superbases—supramolecular systems containing four pyridine subunits. *Tetrahedron Lett.* **2007**, *48*, 261−264.
(24) Bucher, G. DFT Calculations on a New Class of C_3-Symmetric Organic Bases: Highly Basic Proton Sponges and Ligands for Very Small Metal Cations. *Angew. Chem., Int. Ed.* **2003**, *42*, 4039−4042.
(25) Maksić, Z. B.; Glasovac, Z.; Despotović, I. Predicted high proton affinity of poly-2,5-dihydropyrrolimines—the aromatic domino effect. *J. Phys. Org. Chem.* **2002**, *15*, 499−508.
(26) Alder, R. W. Design of C_2-chiral diamines that are computationally predicted to be a million-fold more basic than the original proton sponges. *J. Am. Chem. Soc.* **2005**, *127*, 7924−7931.
(27) Coles, M. P.; Aragón-Sáez, P. J.; Oakley, S. H.; Hitchcock, P. B.; Davidson, M. G.; Maksić, Z. B.; Vianello, R.; Leito, I.; Kaljurand, I.; Apperley, D. C. Superbasicity of a Bis-guanidino Compound with a Flexible Linker: A Theoretical and Experimental Study. *J. Am. Chem. Soc.* **2009**, *131*, 16858−16868.
(28) Oediger, H.; Mőller, F.; Eiter, K. Bicyclic Amidines as Reagents in Organic Syntheses. *Synthesis* **1972**, 591−598.
(29) Tang, J.; Dopke, J.; Verkade, J. G. Synthesis of new exceedingly strong non-ionic bases: RN:P(MeNCH$_2$CH$_2$)$_3$N. *J. Am. Chem. Soc.* **1993**, *115*, 5015−5020 and references therein.
(30) Ishikawa, T.; Isobe, T. Modified Guanidines as Chiral Auxiliaries. *Chem.—Eur. J.* **2002**, *8*, 552−557.
(31) Jessop, P. G.; Heldebrant, D. J.; Li, X. W.; Eckert, C. A.; Liotta, C. L. Reversible nonpolar-to-polar solvent. *Nature* **2005**, *436*, 1102−1102.
(32) Heldebrant, D. J.; Koech, P. K.; Rainbolt, J. E.; Zheng, F.; Smurthwaite, T.; Freeman, C. J.; Oss, I. Leito, Performance of single-component CO_2-binding organic liquids (CO_2BOLs) for post combustion CO_2 capture. *Chem. Eng. J.* **2011**, *171*, 794−800.
(33) Heldebrant, D. J.; Yonker, C. R.; Jessop, P. G.; Phan, L. Organic liquid CO_2 capture agents with high gravimetric CO_2 capacity. *Energy Environ. Sci.* **2008**, *1*, 487−493.
(34) Yang, Z.; He, L.; Zhao, Y.; Li, B.; Yu, B. CO_2 capture and activation by superbase/polyethylene glycol and its subsequent conversion. *Energy Environ. Sci.* **2011**, *4*, 3971−3975.
(35) Lo, R.; Ganguly, B. Efficacy of carbenes for CO_2 chemical fixation and activation by their superbasicity/alcohol: a DFT study. *New J. Chem.* **2012**, *36*, 2549−2554.
(36) Wang, C.; Luo, X.; Luo, H.; Jiang, D.; Li, H.; Dai, S. Tuning the Basicity of Ionic Liquids for Equimolar CO_2 Capture. *Angew. Chem., Int. Ed.* **2011**, *50*, 4918−4922 and references therein.
(37) Zheng, F.; Sa, R.; Cheng, J.; Jiang, H.; Shen, J. Carbocation−π interaction with Car−Parrinello molecular dynamics: Ab initio molecular dynamics investigation of complex of methyl cation with benzene. *Chem. Phys. Lett.* **2007**, *435*, 24−28.
(38) Frontera, A.; Garau, C.; Quiñonero, D.; Ballester, P.; Costa, A.; Deyà, P. M. Unexpected Binding Affinity of [2.2]Paracyclophane to Cations. *Internet Electron. J. Mol. Des.* **2005**, *4*, 264−269.
(39) Frontera, A.; Quiñonero, D.; Garau, C.; Costa, A.; Ballester, P.; Deyà, P. M. Ab initio study of [n.n]paracyclophane (n=2,3) complexes with cations: Unprecedent through-space substituent effects. *J. Phys. Chem. A* **2006**, *110*, 5144−5148.
(40) Vianello, R.; Maksić, Z. B. Rees polycyanated hydrocarbons and related compounds are extremely powerful Brønsted superacids in the gas-phase and DMSO—a density functional B3LYP study. *New J. Chem.* **2008**, *32*, 413−427.
(41) Lewis, N. S.; Nocera, D. G. Powering the planet: Chemical challenges in solar energy utilization. *Proc. Natl. Acad. Sci. U. S. A.* **2006**, *103*, 15729−15735.
(42) Lubitz, W.; Tumas, W. Hydrogen: An Overview. *Chem. Rev.* **2007**, *107*, 3900−3903.
(43) Schlapbach, L.; Züttel, A. Hydrogen-storage materials for mobile applications. *Nature* **2001**, *414*, 353−358.
(44) Zhou, L. Progress and problems in Hydrogen storage methods. *Renewable Sustainable Energy Rev.* **2005**, *9*, 395−408.
(45) Deng, W.-Q.; Xu, X.; Goddard, W. A. New Alkali Doped Pillared Carbon Materials Designed to Achieve Practical Reversible Hydrogen Storage for Transportation. *Phys. Rev. Lett.* **2004**, *92*, 166103−166106.
(46) Li, Y.; Zhou, G.; Li, J.; Gu, B.-L.; Duan, W. Alkali-Metal-Doped B80 as High-Capacity Hydrogen Storage Media. *J. Phys. Chem. C* **2008**, *112*, 19268−19271.
(47) Cheng, H.; Sha, X.; Chen, L.; Cooper, A. C.; Foo, M.-L.; Lau, G. C.; Bailey III, W. H.; Pez, G. P. An Enhanced Hydrogen Adsorption Enthalpy for Fluoride Intercalated Graphite Compounds. *J. Am. Chem. Soc.* **2009**, *131*, 17732−17733.

(48) Baldé, C. P.; Hereijgers, B. P. C.; Bitter, J. H.; de Jong, K. P. Facilitated Hydrogen Storage in $NaAlH_4$ Supported on Carbon Nanofibers. *Angew. Chem., Int. Ed.* **2006**, *45*, 3501−3503.
(49) Lee, H.; Lee, J.-W.; Kim, D. Y.; Park, J.; Seo, Y.-T.; Zeng, H.; Moudrakovski, I. L.; Ratcliffe, C. I.; Ripmeester, J. A. Tuning clathrate hydrates for hydrogen storage. *Nature* **2005**, *434*, 743−746.
(50) Züttel, A.; Borgschulte, A.; Orimo, S. Tetrahydroborates as new hydrogen storage materials. *Scr. Mater.* **2007**, *56*, 823−828.
(51) Weitkamp, J.; Firtz, M.; Ernst, S. Zeolites as media for hydrogen storage. *Int. J. Hydrogen Energy* **1995**, *20*, 967−970.
(52) Orimo, S.; Nakamori, Y.; Eliseo, J. R.; Züttel, A.; Jensen, C. M. Complex Hydrides for Hydrogen Storage. *Chem. Rev.* **2007**, *107*, 4111−4132.
(53) Han, S. S.; Deng, W.-Q.; Goddard, W. A., III. Improved Designs of Metal−Organic Frameworks for Hydrogen Storage. *Angew. Chem., Int. Ed.* **2007**, *46*, 6289−6292.
(54) Furukama, H.; Miller, M. A.; Yaghi, O. M. Independent verification of the saturation hydrogen uptake in MOF-177 and establishment of a benchmark for hydrogen adsorption in metal−organic frameworks. *J. Mater. Chem.* **2007**, *17*, 3197−3204.
(55) Cabria, I.; López, M. J.; Alonso, J. A. Hydrogen storage capacities of nanoporous carbon calculated by density functional and Møller-Plesset methods. *Phys. Rev. B* **2008**, *78*, 075415.
(56) Wu, H.; Zhou, W.; Yildirim, T. Hydrogen Storage in a Prototypical Zeolitic Imidazolate Framework-8. *J. Am. Chem. Soc.* **2007**, *129*, 5314−5315.
(57) Sheppard, D. A.; Buckley, C. E. Hydrogen adsorption on porous silica. *Int. J. Hydrogen Energy* **2008**, *33*, 1688−1692.
(58) Cohen, R. L.; Wernick, J. H. Hydrogen Storage Materials: Properties and Possibilities. *Science* **1981**, *214*, 1081−1087.
(59) Graetz, J. New approaches to hydrogen storage. *Chem. Soc. Rev* **2009**, *38*, 73−82.
(60) Srinivasu, K.; Ghosh, S. K. An *ab Initio* Investigation of Hydrogen Adsorption in Li-Doped closo-Boranes. *J. Phys. Chem. C* **2010**, *115*, 1450−1456.
(61) Pan, S.; Giri, S.; Chattaraj, P. K. A computational study on the hydrogen adsorption capacity of various lithium-doped boron hydrides. *J. Comput. Chem.* **2012**, *33*, 425−434.
(62) Pan, S.; Merino, G.; Chattaraj, P. K. The hydrogen trapping potential of some Li-doped star-like clusters and super-alkali systems. *Phys. Chem. Chem. Phys.* **2012**, *14*, 10345−10350.
(63) Das, R.; Chattaraj, P. K. A (T−P) Phase Diagram of Hydrogen Storage on $(N_4C_3H)_6Li_6$. *J. Phys. Chem. A* **2012**, *116*, 3259−3266.
(64) Pan, S.; Banerjee, S.; Chattaraj, P. K. Role of Lithium Decoration on Hydrogen Storage Potential. *J. Mex. Chem. Soc.* **2012**, *56*, 229−240.
(65) Srinivasu, K.; Ghosh, S. K.; Das, R.; Giri, S.; Chattaraj, P. K. Theoretical investigation of hydrogen adsorption in all-metal aromatic clusters. *RSC Adv.* **2012**, *2*, 2914−2922.
(66) Becke, A. D. Density-Functional Thermochemistry. III. The Role of Exact Exchange. *J. Chem. Phys.* **1993**, *98*, 5648−5652.
(67) Lee, C.; Yang, W.; Parr, R. G. Development of the Colle-Salvetti correlation-energy formula into a functional of the electron density. *Phys. Rev. B* **1988**, *37*, 785−789.
(68) Hehre, W. J.; Radom, L.; Schleyer, P. v. R.; Pople, J. A. *Ab Initio Molecular Orbital Theory*; Wiley: New York, 1988.
(69) Zhao, Y.; Truhlar, D. G. Density Functionals with Broad Applicability in Chemistry. *Acc. Chem. Res.* **2008**, *41*, 157−167.
(70) Tomasi, J.; Persico, M. Molecular Interactions in Solution: An Overview of Methods Based on Continuous Distributions of the Solvent. *Chem. Rev.* **1994**, *94*, 2027−2094.
(71) Cossi, M.; Barone, V.; Cammi, R.; Tomasi, J. Ab Initio Study of Solvated Molecules: a New Implementation of the Polarizable Continuum Model. *Chem. Phys. Lett.* **1996**, *255*, 327−335.
(72) Barone, V.; Cossi, M.; Tomasi, J. A new definition of cavities for the computation of solvation free energies by the polarizable continuum model. *J. Chem. Phys.* **1997**, *107*, 3210−3221.
(73) Barone, V.; Cossi, M.; Tomasi, J. Geometry optimization of molecular structures in solution by the polarizable continuum model. *J. Comput. Chem.* **1998**, *19*, 404−417.
(74) Cossi, M.; Barone, V. Analytical second derivatives of the free energy in solution by polarizable continuum models. *J. Chem. Phys.* **1998**, *109*, 6246−6254.
(75) Camaioni, D. M.; Schwerdtfeger, C. A. Comment on "Accurate Experimental Values for the Free Energies of Hydration of H^+, OH^-, and H_3O^+". *J. Phys. Chem. A* **2005**, *109*, 10795−10797.
(76) Topol, I. A.; Tawa, G. J.; Burt, S. K.; Rashin, A. A. Calculation of Absolute and Relative Acidities of Substituted Imidazoles in Aqueous Solvent. *J. Phys. Chem. A* **1997**, *101*, 10075−10081.
(77) Magill, A. A.; Cavell, K. J.; Yates, B. F. Basicity of Nucleophilic Carbenes in Aqueous and Nonaqueous SolventsTheoretical Predictions. *J. Am. Chem. Soc.* **2004**, *126*, 8717−8724.
(78) Brown, T. N.; Mora-Diez, N. Computational determination of aqueous pK_a values of protonated benzimidazoles. *J. Phys. Chem. B.* **2006**, *110*, 9270−9279.
(79) Trummal, A.; Rummel, A.; Lippmaa, E.; Burk, P.; Koppel, I. A. IEF-PCM Calculations of Absolute pK_a for Substituted Phenols in Dimethyl Sulfoxide and Acetonitrile Solutions. *J. Phys. Chem. A* **2009**, *113*, 6206−6212.
(80) Politzer, P.; Murray, J. S. In *Reviews in Computational Chemistry*; Lipkowitz, K. B.; Boyd, D. B., Eds.; VCH Publishers: New York, 1991; Vol 2, Chapter 7, pp 273−312.
(81) Tomasi, J.; Bonaccorsi, R.; Cammi, R. *Theoretical Models of Chemical Bonding*; Springer: Berlin, 1990; pp 230−268.
(82) Pathak, R. K.; Gadre, S. R. Maximal and minimal characteristics of molecular electrostatic potentials. *J. Chem. Phys.* **1990**, *93*, 1770−1773.
(83) Scrocco, E.; Tomasi, J. Electronic molecular structure, reactivity and intermolecular forces: an euristic interpretation by means of electrostatic molecular potentials. *Adv. Quantum Chem.* **1979**, *11*, 115−193.
(84) Murray, J. S.; Politzer, P. Statistical Analysis of the Molecular Surface Electrostatic Potential: An Approach to Describing Noncovalent Interactions in Condensed Phases. *J. Mol. Struct.: THEOCHEM* **1998**, *425*, 107−114.
(85) Brinck, T.; Murray, J. S.; Politzer, P. Quantative determination of the total local polarity (charge separation) in molecules. *Mol. Phys.* **1992**, *76*, 609−617.
(86) Murray, J. S.; Politzer, P. Electrostatic potentials of amine nitrogens as a measure of the total electron-attracting tendencies of substituents. *Chem. Phys. Lett.* **1988**, *152*, 364−370.
(87) Haeberlein, M.; Murray, J. S.; Brinck, T.; Politzer, P. Calculated electrostatic potentials and local surface ionization energies of para-substituted anilines as measures of substituent effects. *Can. J. Chem.* **1992**, *70*, 2209−2214.
(88) Suresh, C. H. A Molecular Electrostatic Potential Approach to Determine the Steric Effect of Phosphine Ligands in Organometallic Chemistry. *Inorg. Chem.* **2006**, *45*, 4982−4986.
(89) Frisch, M. J.; Trucks, G. W.; Schlegel, H. B.; Scuseria, G. E.; Robb, M. A.; Cheeseman, J. R. J.; Montgomery Jr., A.; Vreven, T.; Kudin, K. N.; Burant, J. C.; et al. *Gaussian 03*, Revision E.01; Gaussian, Inc.: Wallingford, CT, 2004.
(90) Frisch, M. J.; Trucks, G. W.; Schlegel, H. B.; Scuseria, G. E.; Robb, M. A.; Cheeseman, J. R.; Scalmani, G.; Barone, V.; Mennucci, B.; Petersson, G. A.; et al. *Gaussian 09*, Revision B01; Gaussian, Inc: Wallingford, CT, 2010.
(91) Alder, R. W.; Bowman, P. S.; Steele, R. W. S.; Winterman, D. R. The remarkable basicity of 1,8-bis(dimethylamino)naphthalene. *J. Chem. Soc., Chem. Commun.* **1968**, 723−724.
(92) Decouzon, M.; Gal, G. F.; Maria, P. C.; Raczynska, E. D. Superbases in the gas phase: Amidine and guanidine derivatives with proton affinities larger than 1000 kJ mol^{-1}. *Rapid Commun. Mass Spectrum.* **1993**, *7*, 599−602.
(93) Despotović, I.; Maksić, Z. B.; Vianello, R. Design of Bronsted neutral organic bases and superbases by computational DFT methods:

cyclic and polycyclic Quinones and [3]Carbonylradialenes. *Eur. J. Org. Chem.* **2007**, 3402.
(94) Lahann, J.; Höcker, H.; Langer, R. Synthesis of amino[2.2]-paracyclophanes- Beneficial monomers for bioactive coating of medical implant materials. *Angew. Chem., Int. Ed.* **2001**, *40*, 726−728.
(95) Sheehan, M.; Cram, D. J. Macro Rings. XXXIX. Syntheses and Spectral Properties of the Aromatic Monosubstituted Derivatives of [3.3]Paracyclophane. *J. Am. Chem. Soc.* **1969**, *91*, 3544−3552.
(96) Tonner, R.; Heydenrych, G.; Frenking, G. First and Second Proton Affinities of Carbon Bases. *Chem. Phys.Chem.* **2008**, *9*, 1474−1481.
(97) Kaljurand, I.; Rodima, T.; Leito, I.; Koppel, I. A.; Schwesinger, R. Self-consistent spectrophotometric basicity scale in acetonitrile covering the range between pyridine and DBU. *J. Org. Chem.* **2000**, *65*, 6202−6208.
(98) Kovačević, B.; Maksić, Z. B. Basicity of Some Organic Superbases in Acetonitrile. *Org. Lett.* **2001**, *3*, 1523−1526.
(99) Liao, S.-M.; Du, Q.-S.; Meng, J.-Z.; Pang, Z.-W.; Huang, R.-B. The multiple roles of histidine in protein interactions. *Chem. Cent. J.* **2013**, *7*, 44−56.
(100) Tukov, A. A.; Normand, A. T.; Nechaev, M. S. *N*-heterocyclic carbenes bearings two, one and no nitrogen atoms at the ylidene carbon: insight from theoretical calculations. *Dalton Trans.* **2009**, 7015−7028.
(101) Lochan, R. C.; Head-Gordon, M. Computational studies of molecular hydrogen binding affinities: The role of dispersion forces, electrostatics, and orbital interactions. *Phys. Chem. Chem. Phys.* **2006**, *8*, 1357−1370.
(102) Mavrandonakis, A.; Klopper, W. First-Principles Study of Single and Multiple Dihydrogen Interaction with Lithium Containing Benzene Molecules. *J. Phys. Chem. C* **2008**, *112*, 11580−11585.
(103) Parr, R. G.; Chattaraj, P. K. Principle of maximum hardness. *J. Am. Chem. Soc.* **1991**, *113*, 1854−1855.
(104) Chamorro, E.; Chattaraj, P. K.; Fuentealba, P. Variation of the Electrophilicity Index along the Reaction Path. *J. Phys. Chem.* **2003**, *107*, 7068−7072.